

# Magnetic structure of Fe, Mn, and Cr clusters supported on Cu(111)

Anders Bergman,<sup>1,\*</sup> Lars Nordström,<sup>1</sup> Angela Burlamaqui Klautau,<sup>2</sup> Sonia Frota-Pessôa,<sup>3</sup> and Olle Eriksson<sup>1</sup>

<sup>1</sup>*Department of Physics, Uppsala University, Box 530 Sweden*

<sup>2</sup>*Departamento de Física, Universidade Federal do Pará, Belém, PA, Brazil*

<sup>3</sup>*Instituto de Física, Universidade de São Paulo, CP 66318, São Paulo, SP, Brazil*

(Dated: December 2, 2024)

The magnetic structures of small clusters of Fe, Mn, and Cr supported on a Cu(111) surface have been studied with non-collinear first principles theory. Different geometries such as triangles, pyramids and wires are considered and the cluster sizes have been varied between two to ten atoms. The calculations have been performed using a real space linear muffin-tin orbital method. The Fe clusters are found to order ferromagnetically regardless of the cluster geometry. For Mn and Cr clusters, antiferromagnetic exchange interactions between nearest-neighbours are found to cause collinear antiferromagnetic ordering when the geometry allows it. If the antiferromagnetism is frustrated by the cluster geometry non-collinear ordering is found. A comparison between the calculated structures and ground states obtained from simplified Heisenberg Hamiltonians show that the exchange interaction varies for different atoms in the clusters as a result of the different local structure.

PACS numbers: 75.75.+a, 73.22.-f, 75.10.-b

## I. INTRODUCTION

The remarkable progress of experimental methodologies with atomic resolution, such as the scanning electron microscopy<sup>1</sup> (STM), have paved the way for studies of nanoscale magnetic materials such as ad-atoms, clusters and wires deposited on surfaces. As a result of the reduced dimensions and symmetries for such systems, magnetic behaviour that differs from bulk materials can be found<sup>2,3</sup>. This attracts interest not only for the novel physics that can occur in these systems but also for the possibility to tailor the electronic and magnetic properties by changing the structure and the local environment of the systems.

Studies of systems consisting of only a few atoms can give valuable information on how the magnetic structure evolves from single atoms towards the bulk behaviour. Fe, Mn, and Cr are all known to exhibit interesting magnetic behaviour. While being ferromagnetic in the bcc phase, Fe in the fcc phase has been found to exhibit a spin-spiral structure when synthesized as precipitates in a Cu matrix<sup>4</sup> and calculations show that the magnetic structure is strongly dependent on the lattice parameter<sup>5</sup>. Cr has in bulk an incommensurate antiferromagnetic spin density wave<sup>6</sup> which can be tuned by creating superlattices with ferromagnetic or paramagnetic layers and varying the interface roughness and layer thickness<sup>7</sup>. When deposited on stepped surfaces, Cr can be found to have non-collinear ordering<sup>8</sup>. Bulk Mn exhibits perhaps the most intriguing magnetic structure of all elements with a unit cell containing 58 atoms<sup>9</sup> with a complex non-collinear antiferromagnetic magnetic structure.<sup>10</sup>

Free clusters of Fe, Mn, and Cr have been studied both experimentally and theoretically. Stern-Gerlach measurements on Fe<sup>11</sup> clusters show ferromagnetic behaviour while Mn clusters<sup>12</sup> and Cr clusters<sup>13</sup> show varying small net deflections, which can be interpreted as

the result of antiferromagnetic or even non-collinear magnetic configurations. Calculations have shown that small Mn and Cr clusters can exhibit non-collinear magnetic ordering<sup>14,15,16</sup> in agreement with the Stern-Gerlach experiments.

Supported transition metal clusters have also been studied extensively where a majority of the studies have been theoretical. Among the experimental studies, most work has been done on Fe, where Fe clusters deposited on a Ni surface have been found to be ferromagnetic with oscillating magnitude of the orbital moments<sup>17</sup> and Fe clusters supported on a graphite surface have been found to exhibit enhanced spin and orbital moments compared to bulk<sup>18</sup>. Among the theoretical studies, the reported calculations have mostly only considered collinear magnetization densities. Monoatomic wires of Fe on Cu(111) and Cu(001) show ferromagnetic behaviour with a strong magnetic anisotropy<sup>19,20</sup>. Small Mn clusters on Ag(001) have been found to exhibit magnetic bistability<sup>21,22</sup> which is also the case for mixed clusters of FeMn and FeCr that have been found to have both ferro- and antiferromagnetic solutions close in energy<sup>23</sup>. Recent studies have found that dimers of Mn and Cr become non-collinear when deposited on Ni(001)<sup>24</sup> and Fe(001)<sup>25</sup> surfaces due to competing exchange interactions between the cluster atoms and the surface<sup>24</sup>.

In a previous paper<sup>26</sup> we reported on non-collinear magnetic ordering for a selection of small Mn clusters supported on a Cu surface. In this paper we expand these results and present theoretical results concerning the magnetic ordering and interactions for Fe, Mn, and Cr clusters deposited on a Cu(111) surface. The calculations have been performed using the real space linear muffin-tin orbital method (RS-LMTO-ASA), which is a first principles order-N method that has recently been extended to the treatment of non-collinear magnetism<sup>26</sup>.

## II. METHOD

The RS-LMTO-ASA method is based on the LMTO-ASA technique<sup>27</sup> and the Haydock recursion method<sup>28</sup>. The LMTO-ASA formalism provides an efficient, parameter-free, basis set for treating close packed metallic systems and the recursion method gives the ability to treat problems where translational symmetry is absent and does also convey order-N scaling with respect to the number of inequivalent atoms in the systems. The recursion method does not directly solve the eigenvalue problem as formulated in the DFT, but allows one to calculate the local density of states for the orbitals of the atoms in the selected system. The RS-LMTO-ASA method has successfully been used for a wide range of problems including bulk systems, multilayers, embedded impurities and clusters and clusters on surfaces. Earlier and more detailed descriptions of the collinear implementation of the RS-LMTO-ASA can be found elsewhere<sup>29,30</sup>.

In the local spin density approximation (LSDA)<sup>31</sup>, the electron density is expressed through a 2x2 density matrix  $\rho$  which can be expressed in terms of the non-magnetic charge density  $n$  and the magnetization density  $\mathbf{m}$  as  $\rho = (n\mathcal{I} + \mathbf{m} \cdot \boldsymbol{\sigma})/2$  where  $\mathcal{I}$  is the 2x2 identity matrix and  $\boldsymbol{\sigma} = \{\sigma_x, \sigma_y, \sigma_z\}$  are the Pauli matrices. Self-consistent methods<sup>32,33,34</sup> for calculating the electronic structure for non-collinear magnetization densities have existed for quite some time<sup>35</sup>, and here we will focus on the specific details for treating non-collinear magnetization densities within the RS-LMTO-ASA.

With the recursion method, the local density of states  $N(\epsilon)$  where  $\epsilon$  is the energy, is obtained as  $N(\epsilon) = -\frac{1}{\pi} \Im \text{tr} \mathcal{G}(\epsilon)$ . Here  $\mathcal{G}(\epsilon)$  is the local Green's function  $\mathcal{G}(\epsilon) = (\epsilon - \mathcal{H})^{-1}$ , where  $\mathcal{H}$  is the Hamiltonian. Similar to the LDOS, the collinear magnetic density of states  $m(\epsilon)$  can be calculated as  $m(\epsilon) = -\frac{1}{\pi} \Im \text{tr}(\sigma_z \mathcal{G}(\epsilon))$ . Since the Pauli spin matrix  $\sigma_z$  is diagonal in spin-space, the collinear magnetic density of states can be calculated using only diagonal elements of the Green's function. If a generalized non-collinear magnetization density

$$\mathbf{m}(\epsilon) = -\frac{1}{\pi} \Im \text{tr}(\boldsymbol{\sigma} \mathcal{G}(\epsilon)) \quad (1)$$

where  $\boldsymbol{\sigma} = \{\sigma_x, \sigma_y, \sigma_z\}$  is sought, evaluation of the off-diagonal parts of the Green's function is in principle needed. The off-diagonal elements of the Green's function are possible to obtain by performing the recursion starting from carefully selected linear combinations of muffin-tin orbitals<sup>36</sup> or perform a computationally more demanding block recursion calculation<sup>37</sup>. However, in our implementation we avoid the evaluation of off-diagonal elements by applying successive unitary transformations  $\mathcal{U}$  on the Hamiltonian,  $\mathcal{H}' = \mathcal{U} \mathcal{H} \mathcal{U}^\dagger$ . When the Hamiltonian is transformed in this way, the Green's function transform similarly;  $\mathcal{G}' = \mathcal{U} \mathcal{G} \mathcal{U}^\dagger$ .

Using the unitary property  $\mathcal{U}^\dagger \mathcal{U} = 1$  and the fact that cyclic permutations of matrix multiplications conserve

the trace of the product, the generalized magnetic density of states  $\mathbf{m}(\epsilon)$ , can be written as

$$\mathbf{m}(\epsilon) = -\frac{1}{\pi} \Im \text{tr}\{\boldsymbol{\sigma} \mathcal{U}^\dagger \mathcal{U} \mathcal{G} \mathcal{U}^\dagger \mathcal{U}\} = -\frac{1}{\pi} \Im \text{tr}\{\boldsymbol{\sigma}' \mathcal{G}'\}, \quad (2)$$

where  $\boldsymbol{\sigma}'$  is the Pauli matrices after the unitary transformation. The transformation matrix  $\mathcal{U}$  is different for the three directions, and chosen so that,  $\mathcal{U} \sigma_j \mathcal{U}^\dagger = \sigma'_z$ , for  $j = x, y, z$ , to yield a diagonal representation. In the trivial case of  $j = z$  the unitary transformation is just the identity matrix. For the other directions, the unitary transformation corresponds to a spin rotation where  $\mathcal{U}$  can be calculated using spin- $\frac{1}{2}$  rotation matrices. Decomposing the Hamiltonian into a spin-dependent part,  $\mathbf{B}$ , and a spin-independent component,  $H$ , yields that  $\mathcal{U}$  operates only on the spin-dependent part,

$$\mathcal{H}' = H + \mathbf{B} \cdot \mathcal{U} \boldsymbol{\sigma} \mathcal{U}^\dagger. \quad (3)$$

From the transformed Hamiltonians,  $\mathcal{H}'$ , the LDOS for the different directions can then be calculated using the regular recursion method and the magnetic density along the three directions can be obtained. From the three orthogonal directions, the local magnetization axis is calculated and the LDOS for the local spin axis can be constructed by taking the scalar product of the generalized magnetic density of states and the local magnetization vector. As all Hamiltonians are constructed within an *ab initio* LMTO-ASA formalism, all calculations are fully self-consistent, and the spin densities are treated within the local spin density approximation<sup>31</sup>. Since the recursion procedure is performed for three orthogonal directions, the computational cost is tripled compared with the collinear implementation of the RS-LMTO-ASA, but the linear scaling with respect to the number of inequivalent atoms is retained.

The calculations of the transition metal clusters have been performed by embedding the clusters as a perturbation on a self-consistently converged perfect Cu(111) surface. The Cu surface has been calculated using the experimental lattice parameter of Cu. As is usually the case for LMTO-ASA methods, the vacuum outside the surface needs to be simulated by having a number of layers of empty spheres above the Cu surface in order to provide a basis for the wave-function in the vacuum and to treat charge transfers correctly. After embedding the cluster on the surface, the charge and magnetization densities of the cluster atoms and the neighboring Cu atoms and empty spheres are then recalculated until self-consistency is obtained while the electronic structure for atoms far from the cluster are kept unchanged to their unperturbed values. Structural relaxations have not been included in this study, so the cluster sites have been placed on the regular fcc lattice above the Cu surface. Earlier studies on supported transition metal clusters<sup>38</sup> have shown that structural relaxations can change the magnetic properties of the clusters. On the other hand, in an experimental situation, small clusters as those considered in this study

are usually constructed in an out-of-equilibrium situation by manipulation with an STM tip and calculated equilibrium geometries might therefore not be relevant. The most relevant relaxation for these kind of artificially created clusters would be the distance between the cluster atoms and the substrate atoms and since a noble metal substrate is used in this study, the interaction between clusters and substrate play a lesser role compared to the interactions between the cluster atoms. The clean Cu(111) surface has been modeled by a large ( $>5000$ ) slab of atoms and the continued fraction, that occurs in the recursion method, have been terminated with the Beer-Pettifor<sup>39</sup> terminator after 30 recursion levels.

In order to get a simple connection between our calculated magnetic structures and exchange interactions  $J_{ij}$  between the different atoms situated at sites  $i$  and site  $j$ , we map our results into the classical Heisenberg Hamiltonian for certain clusters.

$$\mathcal{H}_{\mathcal{H}} = - \sum_{i,j,i \neq j} J_{ij} \cos \theta_{ij}, \quad (4)$$

where  $\theta_{ij}$  is the angle between the magnetic moment on site  $i$  and site  $j$ . Note that in Eqn. 4, the magnitude of the spins have been incorporated into the effective  $J_{ij}$  interactions. In this work use the Heisenberg Hamiltonian for comparison with our first-principles results by minimizing the angles  $\theta_{ij}$  when the exchange interaction parameters  $J_{ij}$  are set to fixed values. The minimization of the Heisenberg Hamiltonian is performed by a genetic algorithm<sup>40</sup>.

### III. RESULTS

#### A. Fe clusters

In Fig. 1 the magnetic structure of several Fe clusters are shown. Regardless of the geometry of the Fe clusters, we find the magnetic ordering in the clusters to always be ferromagnetic. The collinear magnetic structure, which can be put in contrast with the non-collinear ordering found for fcc structured Fe clusters embedded in bulk Cu<sup>4</sup>, could be caused by the fact that the decreased coordination of the surface clusters lead to a high-spin state which favours ferromagnetic coupling between neighbouring Fe atoms<sup>41</sup>. This is also consistent with an analysis by Lizarraga *et al.*<sup>42</sup>.

The magnetic moments for the Fe atoms in the clusters shown in Fig. 1 range between  $3.4 \mu_B$  for the atoms in the dimer to  $2.6 \mu_B$  for the central atom in the seven atom cluster displayed in Fig. 1(d). It has been shown for Co clusters in Cu(001)<sup>30</sup> and Fe clusters on Ni and Cu surfaces<sup>43</sup>, that the magnetic moment has a linear dependence of the number of cluster neighbors around the atom. The magnetic moments of the Fe clusters on Cu(111) of Fig. 1 show a similar trend and depend almost linearly on the number of nearest Fe neighbours. Therefore, the strong correlation between the magnetic

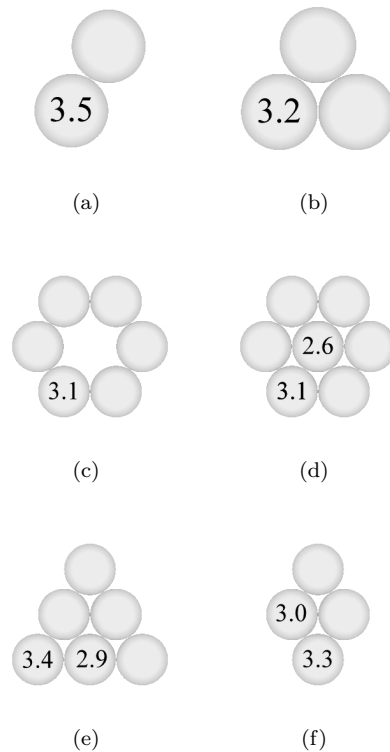


FIG. 1: The geometries for clusters of Fe atoms on a Cu(111) surface. All Fe clusters are found to exhibit a ferromagnetic ground state regardless of the cluster structure. The numbers indicate the atom projected spin moment of the different atoms.

moment for the atoms in the Fe clusters and the number of Fe neighbours can be used to predict the total magnetic moment of any Fe cluster as long as the shape is determined and the cluster is planar. This would indicate that the magnetic moment per atom for a perfect monolayer of Fe atoms on a Cu(111) surface would be  $\sim 2.6 \mu_B$  which is in good agreement with earlier calculations of Fe monolayers on Cu<sup>44,45,46,47</sup>. Our findings of ferromagnetic coupling indicate that a single Fe monolayer would be ferromagnetic in agreement with Ref. 45 whereas Ref. 44 found that a single row antiferromagnetic order would be the most stable magnetic configuration. This discrepancy may be explained by the use of different lattice parameters in Refs. 45 and 44.

#### B. Mn clusters

In a previous paper<sup>26</sup> we showed that due to antiferromagnetic coupling between nearest neighbour atoms in Mn clusters deposited on Cu one finds either a collinear antiferromagnetic structure or, if frustration occurs due to the cluster geometry, a non-collinear magnetic structure. A collection of frustrated cluster geometries with

triangular shapes is shown in Fig. 2. For the equilateral triangle in Fig. 2(a) a non-collinear arrangement with angle of  $120^\circ$  between the magnetic moments is the most stable configuration. The isosceles triangle shown in Fig. 2(b) has an antiferromagnetic collinear ground state which indicates that the exchange coupling between the two Mn atoms furthest from each other is either very small compared to the antiferromagnetic nearest-neighbour exchange coupling or has an opposite sign (i.e. ferromagnetic). As the size of the triangles in-

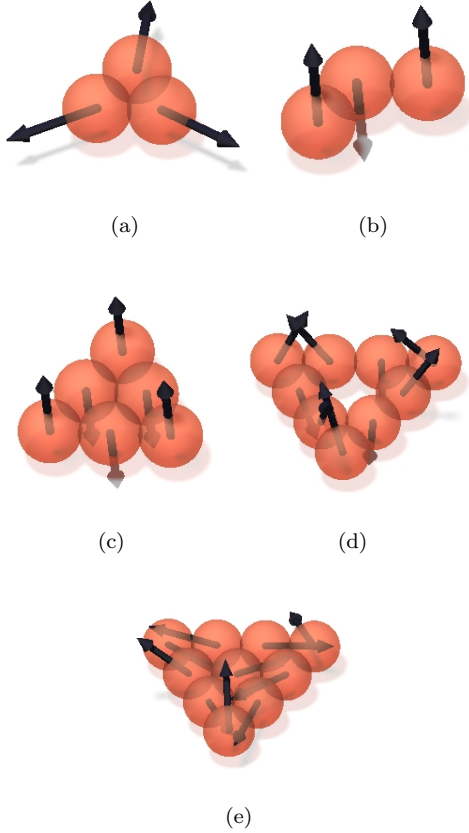


FIG. 2: The magnetic ordering for Mn triangles on a Cu(111) surface. For all geometries except the isosceles triangle shown in (b) and the six atom triangle in (c), non-collinear solutions are obtained due to magnetic frustration.

creases (Figs. 2(c) to 2(e)), the behaviour becomes more intricate. Although the six-atom triangle (Fig. 2(c)) by the analogous geometry as the three atom triangle in Fig. 2(a), could be expected to align in a structure with  $120^\circ$  between neighbouring atoms, it is in fact a collinear antiferromagnetic order that is the most stable solution. The cause for this is the different environment for the corner atoms who only have two nearest neighbours compared to the three central atoms who have four nearest neighbours each. The reduced coordination for the corner atoms causes their antiferromagnetic exchange coupling to nearest neighbours to be enhanced. A similar

mechanism can be found for the nine-atom cluster displayed in Fig. 2(d), but for this geometry the atoms that are not situated at the corners of the triangle have three nearest neighbours due to the hole in the middle of the cluster. Therefore the difference in the local geometry is smaller between the corner atoms and the central atoms which leads to a more delicate balance of the exchange couplings resulting in a canted antiferromagnetic ground state structure. Compared to the collinear antiferromagnetic geometry, the angles are tilted by  $\sim 30^\circ$ . The analysis of the final ten-atom triangle shown in Fig. 2(e) becomes even more complicated since this cluster has three inequivalent sites; the three corner atoms, the six atoms neighbouring to the corner atoms and the central atom. The ground state magnetic structure for this cluster can be said to be inbetween the  $120^\circ$  structure and the pure antiferromagnetic structure. The influence of the different number of neighbours can be seen in the magnetic moments for the different atoms where the corner atoms have a magnetic moment of  $4.3\mu_B$ , the central atom has  $2.8\mu_B$  and the magnetic moment for the remaining six atoms is  $3.7\mu_B$ .

Nanowires constitute a group of nanostructures that has attracted a lot of attention<sup>3,48,49</sup>. We have calculated the magnetic structure for wires of Mn atoms with lengths between two to nine atoms. The wires are oriented along a  $1\bar{1}0$  direction on the Cu surface. For the dimer and trimer only a collinear antiferromagnetic solution is found. Whereas, for certain longer chains a slightly canted non-collinear order is also found, although it is not always the most stable solution. In Fig. 3 we show the canted magnetic structure for the five-atom wire, the pentamer, which is the only wire where a non-collinear solution is found to be the most stable magnetic configuration. The non-collinear configuration for the pentamer has an angle between an edge atom and its nearest neighbour that is  $170^\circ$  and between two neighbouring central atoms the angle is  $155^\circ$ . The energy difference between the non-collinear and the antiferromagnetic solutions for the pentamer is 8 meV. It is interesting that the calculations yield a non-collinear ground state in spite of the fact that no frustration is present for this geometry. For the longer wires, the deviation from the collinear solutions are smaller both in energy and in the angular difference.

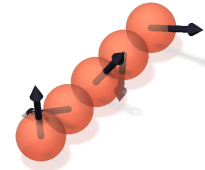


FIG. 3: Calculated magnetic configurations for a five atomic Mn wire, oriented along a  $(1\bar{1}0)$  direction on a Cu(111) surface.

The total energy differences, per cluster atom, between

the antiferromagnetic and the ferromagnetic magnetic configurations for the Mn nanowires are shown in Fig. 4. A large energy difference of 96 meV per atom is found for the dimer whereas the energy differences for the longer wires are significantly smaller. One explanation for the behaviour in Fig. 4 and the higher energy difference for the dimer can be given by considering only nearest neighbour exchange interactions. The atoms in the dimer have only one nearest neighbour, which can cause a larger exchange coupling to the other atom, whereas the longer wires have an increasing number of atoms with two nearest neighbour each. In the case of only nearest-neighbour exchange interactions, the slope of the energy differences in Fig. 4 should scale approximately as  $\frac{1}{N}$  towards a fixed value corresponding to the exchange coupling strength between two atoms with two nearest neighbours each. For the longer wires in Fig. 4, this trend is actually quite well reproduced. There is however an interesting fact that the three atom wire has a smaller energy difference per atom compared to the four atom wire.

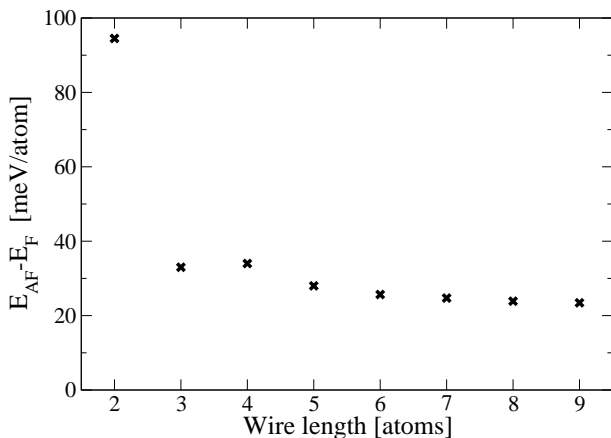


FIG. 4: Total energy differences between antiferromagnetic,  $E^{\text{AF}}$ , and ferromagnetic,  $E^{\text{FM}}$ , configurations of wires of Mn atoms, oriented along a  $(\bar{1}\bar{1}0)$  direction on a Cu(111) surface.

As mentioned before, non-collinear behaviour is found for the cluster in Fig. 3 even though no frustration is present. A probable cause for the non-collinearity is competing ferromagnetic and antiferromagnetic exchange interactions between the different atoms in the cluster. Since the nearest-neighbour interactions are always antiferromagnetic for the Mn clusters (at least for the nearest-neighbour distance used in this study), more long-range interactions must play a role in destabilizing the collinear magnetic state. In order to examine the size and range of the exchange interactions, we have calculated exchange coupling parameters  $J_{ij}$  for the five atom wire shown in Fig. 3. The exchange coupling parameters have been calculated by using the Liechtenstein formula<sup>50</sup> as implemented in the RS-LMTO-ASA<sup>51</sup>, on a collinear solution for the pentamer. The values of the exchange parameters are shown in Table I where the  $i$  and  $j$  are chosen so that site 1 and 5 are the edge atoms and site

TABLE I: Calculated exchange parameters  $J_{ij}$  (in meV) for the Mn pentamer shown in Fig. 3.

| $i \backslash j$ | 1    | 2   | 3    | 4   | 5    |
|------------------|------|-----|------|-----|------|
| 1                | -    | -34 | -5.0 | 6.3 | -3.6 |
| 2                | -34  | -   | -12  | -11 | 6.3  |
| 3                | -5.0 | -12 | -    | -12 | -5.0 |
| 4                | 6.3  | -11 | -12  | -   | -34  |
| 5                | -3.6 | 6.3 | -5.0 | -34 | -    |

3 is the central atom. Hence site 2 is nearest neighbour to site 1 and 3 and the nearest neighbours for site 4 is site 3 and 5. It may be observed that the exchange interactions are strongest and antiferromagnetic between nearest neighbours, with a smaller long range interaction that oscillates between ferromagnetic and antiferromagnetic coupling. The largest magnitude for the exchange interaction is obtained for  $J_{12}$  and  $J_{45}$ , i.e. between an edge atom and its nearest neighbour. Furthermore, Table I shows that although the nearest neighbour interactions have the largest magnitude, the more long ranged interactions always seem to counteract the nearest neighbour interactions. This might not be obvious from the values in Table I but as a clarifying example we can examine the exchange interactions between atom 1 and the other atoms. The negative nearest neighbour interactions in the pentamer would prefer an antiferromagnetic order so that atom 1 would be ferromagnetically coupled to atom 3 and atom 5, and antiferromagnetically coupled to atoms 2 and 4. However, the calculated exchange interactions in Table I show that the  $J_{13}$  and  $J_{15}$  are in fact negative while  $J_{14}$  is positive, thus competing against the antiferromagnetic nearest-neighbour ordering, which results in the non-collinear magnetic state shown in Fig. 3.

### C. Cr clusters

In Fig. 5 the geometries and calculated magnetic configurations for a selection of Cr clusters are shown. Calculations for Mn clusters with similar geometries can be found elsewhere.<sup>26</sup> The magnetic structures are for most of the clusters quite similar to the calculated magnetic structure for Mn clusters although certain differences occur, as will be commented on below. The cluster in Fig. 5(a) has a collinear antiferromagnetic ground state since the edge atoms only have one nearest neighbour and therefore no frustration occurs. The pentamer in Fig. 5(b) also exhibits an antiferromagnetic ground-state, which in contrast to the non-collinear behaviour of the Mn pentamer, is purely collinear. This finding indicates that the magnetic structures of the Cr clusters are more strongly dependant on the nearest-neighbour exchange coupling than the Mn clusters are. The calculated exchange parameters  $J_{ij}$  for the Cr pentamer is shown in Table II. Compared with the exchange interactions for the Mn pentamer in Table I we see that the nearest-

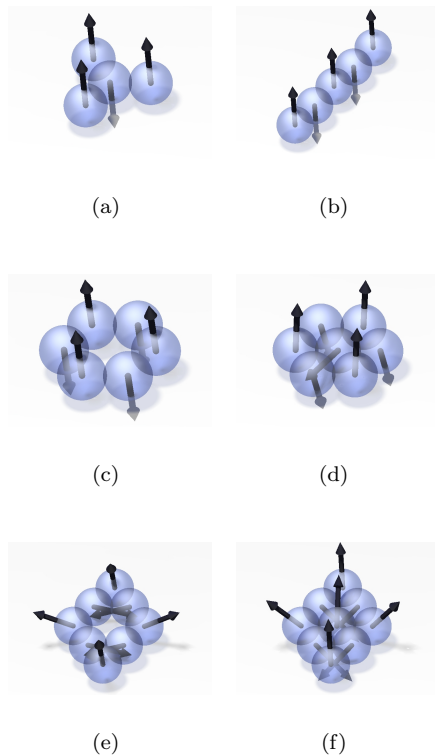


FIG. 5: The calculated magnetic ground state for Cr clusters on a Cu(111) surface.

TABLE II: Calculated exchange parameters  $J_{ij}$  (in meV) for the Cr pentamer shown in Fig. 5(b).

| $i \backslash j$ | 1    | 2     | 3     | 4     | 5    |
|------------------|------|-------|-------|-------|------|
| 1                | -    | -143  | 4.6   | 18.9  | 15.3 |
| 2                | -143 | -     | -97.0 | -40.5 | 18.9 |
| 3                | 4.6  | -97.0 | -     | -97.0 | 4.6  |
| 4                | 18.9 | -40.5 | -97.0 | -     | -143 |
| 5                | 15.3 | 18.9  | 4.6   | -143  | -    |

neighbour interactions are indeed larger between the Cr atoms. On the other hand, the more long ranged interactions also have larger magnitudes in the Cr pentamer than for the Mn counterpart. The exchange interactions between atoms further from each other do however not always compete against the nearest-neighbour interactions as was the case for the Mn pentamer.

The collinear antiferromagnetic behaviour found for the pentamer also occurs for the six atom ring displayed in Fig. 5(c). The cluster in Fig. 5(d) has a symmetric non-collinear ground state with an angle between two neighbouring atoms on the rim of the cluster of  $157^\circ$  and between the central atom and any outer atom the angle is  $101^\circ$ . This can be compared with the energy minima obtained when minimizing the nearest-neighbour Heisenberg Hamiltonian where all nearest neighbour  $J_{ij}$ 's are

set to be negative but equal. The Heisenberg model would give equilibrium angles of the same cluster geometry of between  $151^\circ$  outer neighbours and  $104^\circ$  between the central atom and any neighbour. Although the agreement between our calculated ground state and the Heisenberg minimum is good, it should be noted that due to the difference in the local structure around the central and outer atoms the exchange parameters  $J_{ij}$  should be different between two outer atoms compared to  $J_{ij}$ 's connecting to the central atom. This difference can be considered in a simple model analysis by damping the strength of the exchange parameters where the central atom is connected, and for a damping of 20% for these exchange parameters, the Heisenberg Hamiltonian approach yields an energy minimum with the angles of  $157^\circ$  for neighbouring outer atoms and  $101^\circ$  between the central atom and an edge atom which are in perfect agreement with our calculated angles.

Since the atoms of the hollow cluster in Fig. 5(e) do not all have only two nearest neighbours, as is the case for the other ring like geometry of Fig. 5(c), the cluster can not have an unfrustrated antiferromagnetic solution. Describing the cluster with a Heisenberg Hamiltonian with equal and negative  $J_{ij}$ 's would yield a ground state with  $120^\circ$  between neighbouring atoms. As seen in Fig. 5(e) our calculated magnetic structure differs from the Heisenberg minimum, it is instead described with three different nearest-neighbour angles. The upper and lower edge atoms have an angle of  $113^\circ$  to their neighbours while the leftmost and rightmost of the atoms have an angle of  $170^\circ$  to their nearest neighbours. The third angle is that between two atoms with three neighbours each and they have an angle of  $134^\circ$  between them. This structure can be explained in a similar way as the cluster in Fig. 5(d) could, with different local geometries resulting in different strengths of the exchange coupling and thus different  $J_{ij}$ 's for different atoms.

Filling the empty site in the middle of the cluster in Fig. 5(e) gives the cluster geometry shown in Fig. 5(f). This additional atom causes the magnetic structure to be even more complex. Since the symmetry is lowered compared to the cluster in Fig. 5(d), the central atom does not have the same angle towards all of its neighbours. Instead two angles are needed to describe the structure of the neighbours of the central atom. One of these is the angle of  $69^\circ$  which the central atom makes towards the leftmost and rightmost atoms and the other angle connects the central atom with the remaining four neighbours and the size of this angle is  $128^\circ$ . The upper and lower edge atoms makes an angle of  $136^\circ$  with their neighbours.

#### D. Three dimensional clusters

So far the studied clusters have all been confined in one layer above the Cu surface. However, our method can treat three dimensional clusters as well. In order to



demonstrate this we show the obtained magnetic configurations for a pyramid-like tetrahedron shaped cluster in Fig. 6. As expected from the results for Fe clusters

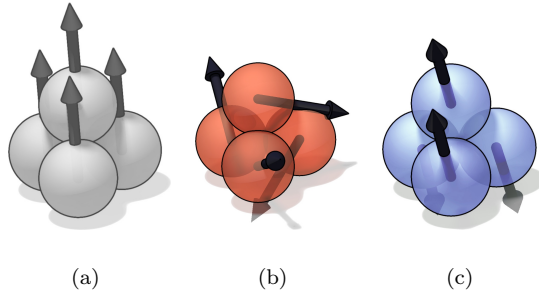


FIG. 6: The calculated magnetic ordering for pyramid shaped clusters on a Cu(111) surface. Fig. 6(a) shows a Fe cluster with a ferromagnetic solution. Fig. 6(b) shows a Mn cluster and Fig. 6(c) shows the Cr pyramid.

reported earlier in this work, the Fe cluster (Fig. 6(a)) exhibits a ferromagnetic order. The atom situated on top of the pyramid has a magnetic moment of  $3.40\mu_B$  while the three Fe atoms closer to the Cu surface have a magnetic moment of  $3.11\mu_B$ . For the Mn cluster shown in Fig. 6(b), a non-collinear structure is found and for the Cr pyramid, shown in Fig. 6(c) a collinear antiferromagnetic solution is found. A model Heisenberg Hamiltonian, as in Eqn. 4, with only antiferromagnetic nearest-neighbour exchange parameters,  $J_{ij}$ , yields a two-fold degenerate ground state, either a collinear antiferromagnet or a non-collinear tetragonal configuration with  $109^\circ$  between neighbouring angles. The calculation for the Mn pyramid over Cu(111) shows angles which are slightly distorted relative to those of the free pyramid, around  $116^\circ$  degrees between the base atoms close to the substrate and angles of about  $100^\circ$  degrees between the base site and the top one. It is peculiar that the Mn cluster has the non-collinear tetragonal configuration as the ground state whereas the Cr cluster has the collinear antiferromagnetic ground state solution. A possible explanation for the non-collinear ground state of the Mn pyramid could be that, similar to the situation for several of the planar clusters, the reduced neighbour coordination for the top atom compared to the atom in the base of the pyramid yields different exchange interaction strengths between the atoms in the cluster. The calculated exchange parameters confirm this since the exchange interaction between a top and a base atom is  $-83$  meV while the interaction between two base atoms  $-46$  meV. However, the situation with different exchange parameters is also present for the Cr pyramid where the interaction strength

between the top atom and a base atom is  $-171$  meV compared to  $-98$  meV for the coupling between two base atoms. This indicates that the bilinear exchange terms  $J$  cannot always describe the magnetic interactions between the atoms in supported magnetic clusters, a fact which previously been suggested for magnetic dimers on surfaces.<sup>52</sup> It can be noted that the difference in the total energy between the non-collinear ground state structure and the antiferromagnetic solution for the Mn cluster is  $25$  meV per atom while the corresponding difference for the Cr pyramid is  $-15$  meV per atom.

#### IV. CONCLUSIONS

We have studied the magnetic structure of small clusters of Fe, Mn, and Cr supported on a Cu(111) surface with non-collinear, first principles calculations. The studied Fe clusters are found to order ferromagnetically regardless of the cluster geometry. For Mn and Cr clusters, antiferromagnetic exchange interactions between nearest-neighbours are found to cause either collinear antiferromagnetic ordering or non-collinear ordering. The non-collinear ordering occurs when the cluster geometry is such that an antiferromagnetic arrangement becomes frustrated. The calculations have been accompanied by comparison with ground states obtained from a simplified Heisenberg Hamiltonian and the comparison shows that the exchange interactions vary for different atoms in the clusters as a result of the different local structure. Differences between the magnetic ordering for Mn and Cr clusters are found where Cr clusters seem to prefer collinear solutions to a higher degree while Mn clusters can exhibit non-collinear configurations even for unfrustrated cluster geometries. Comparisons with model Hamiltonians show that the magnetic structure of certain clusters can be explained by a simple nearest-neighbour Heisenberg Hamiltonian while other cluster geometries cause more complex behaviours.

#### V. ACKNOWLEDGEMENTS

We acknowledge financial support from the Göran Gustafsson foundation, the Swedish Research Council, the Swedish Foundation for Strategic Research, and CNPq, Brazil. The calculations were performed at the high performance computing centers UPPMAX, NSC and HPC2N within the Swedish National Infrastructure for Computing and at the computational facilities of the LCCA, University of São Paulo and of the CENAPAD at University of Campinas, SP, Brazil.

\* Electronic address: Anders.Bergman@fysik.uu.se

<sup>1</sup> G. Binnig and H. Rohrer, *Helv. Phys. Acta.* **55**, 726 (1982).

- <sup>2</sup> F. J. Himpsel, J. E. Ortega, G. J. Mankey, and R. F. Willis, *Adv. Phys.* **47**, 511 (1998).
- <sup>3</sup> P. Gambardella, M. Blanc, K. Kuhnke, K. Kern, F. Picaud, C. Ramseyer, C. Girardet, C. Barreteau, D. Spanjaard, and M. C. Desjonqueres, *Phys. Rev. B* **64**, 045404 (2001).
- <sup>4</sup> Y. Tsunoda, *Journal of Physics: Condensed Matter* **1**, 10427 (1989).
- <sup>5</sup> E. Sjöstedt and L. Nordström, *Phys. Rev. B* **66**, 014447 (2002).
- <sup>6</sup> E. Fawcett, *Rev. Mod. Phys.* **60**, 209 (1988).
- <sup>7</sup> P. Bodeker, A. Schreyer, and H. Zabel, *Phys. Rev. B* **59**, 9408 (1999).
- <sup>8</sup> R. Robles, E. Martinez, D. Stoeffler, and A. Vega, *Phys. Rev. B* **68**, 094413 (2003).
- <sup>9</sup> A. Bradley and J. Thewlis, *Proc. R. Soc. London* **115**, 465 (1927).
- <sup>10</sup> D. Hobbs, J. Hafner, and D. Spisak, *Phys. Rev. B* **68**, 014407 (2003).
- <sup>11</sup> I. M. L. Billas, J. A. Becker, A. Chatelain, and W. A. de Heer, *Phys. Rev. Lett.* **71**, 4067 (1993).
- <sup>12</sup> M. B. Knickelbein, *Phys. Rev. Lett.* **86**, 5255 (2001).
- <sup>13</sup> D. C. Douglass, J. P. Bucher, and L. A. Bloomfield, *Phys. Rev. B* **45**, 6341 (1992).
- <sup>14</sup> C. Kohl and G. F. Bertsch, *Phys. Rev. B* **60**, 4205 (1999).
- <sup>15</sup> T. Morisato, S. N. Khanna, and Y. Kawazoe, *Phys. Rev. B* **72**, 014435 (2005).
- <sup>16</sup> R. C. Longo, E. G. Noya, and L. J. Gallego, *Phys. Rev. B* **72**, 174409 (2005).
- <sup>17</sup> J. T. Lau, A. Fölsch, R. Nietubyc, M. Reif, and W. Wurth, *Phys. Rev. Lett.* **89**, 057201 (2002).
- <sup>18</sup> C. Binns, K. W. Edmonds, S. H. Baker, S. C. Thornton, and M. D. Upward, *Scripta Mater.* **44**, 1303 (2001).
- <sup>19</sup> D. Spisak and J. Hafner, *Phys. Rev. B* **65**, 235405 (2002).
- <sup>20</sup> B. Lazarovits, L. Szunyogh, P. Weinberger, and B. Ujfalussy, *Phys. Rev. B* **68**, 024433 (2003).
- <sup>21</sup> V. S. Stepanyuk, W. Hergert, P. Rennert, K. Wildberger, R. Zeller, and P. H. Dederichs, *J. Magn. Magn. Matter* **165**, 272 (1997).
- <sup>22</sup> V. S. Stepanyuk, W. Hergert, K. Wildberger, S. K. Nayak, and P. Jena, *Surf. Sci.* **384**, L892 (1997).
- <sup>23</sup> V. S. Stepanyuk, W. Hergert, P. Rennert, K. Kokko, A. F. Tatarchenko, and K. Wildberger, *Phys. Rev. B* **57**, 15585 (1998).
- <sup>24</sup> S. Lounis, P. Mavropoulos, P. H. Dederichs, and S. Blügel, *Phys. Rev. B* **72**, 224437 (2005).
- <sup>25</sup> R. Robles and L. Nordström, unpublished.
- <sup>26</sup> A. Bergman, L. Nordström, A. Burlamaqui Klautau, S. Frota-Pessôa, and O. Eriksson, *Phys. Rev. B* **73**, 174434 (2006).
- <sup>27</sup> O. K. Andersen, *Phys. Rev. B* **12**, 3060 (1975).
- <sup>28</sup> R. Haydock, *Solid State Physics* (Academic, New York, 1980), vol. 35, p. 216.
- <sup>29</sup> S. Frota-Pessôa, *Phys. Rev. B* **46**, 14570 (1992).
- <sup>30</sup> A. Klautau and S. Frota-Pessôa, *Surf. Sci.* **579**, 27 (2005).
- <sup>31</sup> V. von Barth and L. Hedin, *J. Phys. Chem.* **5**, 1629 (1972).
- <sup>32</sup> J. Kübler, K.-H. Höck, J. Sticht, and A. R. Williams, *J. Phys. F* **18**, 469 (1988).
- <sup>33</sup> L. M. Sandratskii and P. G. Guletskii, *J. Phys. F* **16**, L43 (1986).
- <sup>34</sup> L. Nordström and D. J. Singh, *Phys. Rev. Lett.* **76**, 4420 (1996).
- <sup>35</sup> L. Sandratskii, *Adv. Phys.* **91**, 47 (1998).
- <sup>36</sup> H. M. Petrilli and S. Frota-Pessôa, *J. Phys. Condens. Matter* **2**, 135 (1990).
- <sup>37</sup> K. K. Saha and A. Mookerjee, *J. Phys. Condens. Matter* **17**, 287 (2005).
- <sup>38</sup> S. Pick, V. S. Stepanyuk, A. N. Baranov, W. Hergert, and P. Bruno, *Phys. Rev. B* **68**, 104410 (2003).
- <sup>39</sup> N. Beer and D. Pettifor, *The Electronic Structure of Complex Systems* (Plenum Press, New York, 1984).
- <sup>40</sup> I. G. Tsoulos and I. E. Lagaris, *Comp. Phys. Comm.* **174**, 152 (2006).
- <sup>41</sup> B. Ujfalussy, L. Szunyogh, and P. Weinberger, *Phys. Rev. B* **54**, 9883 (1996).
- <sup>42</sup> R. Lizarraga, L. Nordström, L. Bergqvist, A. Bergman, E. Sjöstedt, P. Mohn, and O. Eriksson, *Phys. Rev. Lett.* **93**, 107205 (2004).
- <sup>43</sup> P. Mavropoulos, S. Lounis, R. Zeller, and S. Blügel, *Appl. Phys. A* **82**, 103 (2006).
- <sup>44</sup> D. Spisak and J. Hafner, *Phys. Rev. B* **67**, 134434 (2003).
- <sup>45</sup> P. Krüger, M. Taguchi, and S. Meza-Aguilar, *Phys. Rev. B* **61**, 15277 (2000).
- <sup>46</sup> O. Hjortstam, J. Trygg, J. M. Wills, B. Johansson, and O. Eriksson, *Phys. Rev. B* **53**, 9204 (1996).
- <sup>47</sup> G. W. Fernando and B. R. Cooper, *Phys. Rev. B* (1988).
- <sup>48</sup> B. Ujfalussy, B. Lazarovits, L. Szunyogh, G. M. Stocks, and P. Weinberger, *Phys. Rev. B* **70**, 100404 (2004).
- <sup>49</sup> H. J. Lee, W. Ho, and M. Persson, *Phys. Rev. Lett.* **92**, 186802 (2004).
- <sup>50</sup> A. I. Liechtenstein, M. I. Katsnelson, V. P. Antropov, and V. A. Gubanov, *J. Magn. Magn. Matter* **67**, 65 (1987).
- <sup>51</sup> S. Frota-Pessôa, R. B. Muniz, and J. Kudrnovsky, *Phys. Rev. B* **62**, 5293 (2000).
- <sup>52</sup> J. A. T. Costa, R. B. Muniz, and D. L. Mills, *Phys. Rev. Lett.* **94**, 137203 (2005).